

05,08

Control of spin wave properties in bioactive systems based on YIG metasurfaces/ordered polymer films with magnetic microreservoirs

© F.E. Garanin, A.B. Khutieva, M.V. Lomova, A.V. Sadovnikov

Saratov National Research State University,
Saratov, Russia

E-mail: garaninfedorwork@mail.ru

Received May 28, 2024 Revised August 1, 2024

Accepted August 2, 2024

In this paper, we propose configurations of a magnonic microwave guide with a two-dimensional array of magnetic elements located on the surface of the microwave guide. Using the micromagnetic modeling method based on the numerical solution of the Landau–Lifshitz–Gilbert equation, we show the possibility of controlling the characteristics of spin wave (SW) propagation in a structure with polymer planar ordered microreservoirs based on a yttrium iron garnet (YIG) film on a gallium gadolinium garnet (GGG) substrate by changing the configuration of the structure, varying the direction of the magnetization field and changing the magnetization of the magnetic material inside the microreservoir. It is shown that the proposed configurations of magnonic structures allow implementing methods for controlling spin-wave signals, which can find application in magnonic logic devices and sensorics of bioactive materials.

Keywords: spin wave, micromagnetic modeling, microreservoirs, magnetic nanoparticles.

DOI: 10.61011/PSS.2024.09.59216.139

1. Introduction

Spin waves (SW) with wavelength from millimeters to nanometers in gigahertz and subterahertz frequency ranges [1–4] can be basis of new approach of „alternate electronics“ to implement high-speed calculations and processing of signals at micro- and nanolevel. At the same time the characteristics of spin waves (SWs) spreading via magnonic microwave structures can be varied by change in set of parameters that can be divided into different classes. The first class of parameters comprises geometry of waveguide structure (e. g., type of symmetry); the second class — variables (direction and value of external magnetic field H_0 , field of exchange interaction and anisotropy of the material [2]), included in the effective field H_{eff} under framework of the approach accepted to describe the magnetization dynamics, namely solutions of Landau–Lifshitz–Gilbert equation [5]; third class — interphase properties that comprise heterogeneous distribution of magnetization inside the waveguide or adjacent magnetic phase from top and/or in the direct vicinity of the magnonic waveguide [6,7]. The latter class of parameters is used as basis of the universal method of surface view change of magnetic film and as alternate method of control the spin-wave properties, e.g., by making metasurfaces based on yttrium-iron garnet (YIG) — films with low losses, decorated with magnetic structures [8–11].

The hybrid quantum systems, being basis of magnonic, microwave, optical and mechanical devices, have unique properties: wide range of frequency re-adjustment, low level of magnetic decay, large nonlinearity and internal

nonreciprocity [12]. Besides, remember, that change of SW properties can be basis of very sensitive method of description of magnetic materials interaction with environment. So, magnetic YIG waveguides can be used as sensitive magnetoelectric sensors, for example, to early detection of low concentrations of gaseous hydrogen [13–15]. Area of application of magnetic YIG and gadolinium-gallium garnet (GGG) sensors increases and also finds can be applied as biosensors [16]. The hybrid structures, that use giant magnetic impedance [17], ensure production of sensors with high sensitivity to detect cancer markers [18] and inflammatory proteins [19], production of universal coatings to detect different diseases using antibodies [20,21]. 3D-design of magnetic structures is very important, as ensures the surface increasing of sensor contact with environment, which properties shall be measured. So, formation of bulk magnetic microstructures can be basis of new approach during development of high effective sensors based on YIG.

Synthesis of magnetic nanostructures with reproducible parameters is new problem in the material engineering, biomedicine and electronics [22]. Planar polymer microreservoirs are biologically used, in particular, growth of neuroblastoma cells on polymer surface with simultaneous release of active substances from the microreservoirs during their destruction by laser radiation is shown [23]; release of low molecular weight substance under the action of hydrolases from polymer microreservoirs is shown [24], the surface of ophthalmic contact lenses was coated with a polymer coating with microreservoirs to obtain depot-systems with prolonged release of drugs for the eyes treat-

ment [25]. Using laser radiation the intravital drug release from polymeric planar microreservoirs using mouse vessels as an example is shown [26] and other. Besides, films with hollow 3D-containers (chambers) demonstrate sensitivity to VHF-range, this ensures formation of feedback systems and basis of organic electronics for accurate delivery of drugs and/or neurotransmitters [27]. Magnetic nanoparticles (MNP) are widely used to manufacture flat nanocomposite coatings, and are frequently used during drugs delivery [28]. Exhibition of high-frequency magnetic properties of the polymer, with embedded MNP with variation of their bulk portion was detected by experiments using Mandelstam–Brillouin spectroscopy [29]. At the same time introduction of nanoparticles of iron oxide into the polymer matrices ensures to purposefully vary the physical properties of nanocomposites and ensure their sensitivity to electromagnetic effects [30]. The polymer microreservoirs, additionally to depot-release of drug, also demonstrate the sensitivity to UV-radiation, and to radiowaves [31–34]. 3D-biocompatible biodegradable polymer coatings with/without inclusions of metal nanoparticles are successfully used for biotechnological and medical applications, and are good candidates for new biosensor devices with feedback.

To solve problem of implementation of controllable modes of spreading the spin-wave signal the present paper suggests configuration of magnonic microwaveguide based on film YIG/GGG with two-dimensional array of magnetic elements of magnetite based on example of polymer film with ordered magnetic microreservoirs. The method of micromagnetic modeling shows the possibility to control the characteristics of SWs spreading based of making the spatial distributions of magnetization and spectral power density of signal in the output section of the considered structure. Two structure configurations and transformation of electrons of signal passage upon variation of direction of bias field are discussed.

2. Description of studied structure and numerical model

The micromagnetic modeling [35] was performed for different configurations of lattice of irregular magnonic structure with microreservoirs (Figures 1,2). YIG ($Y_3Fe_5O_{12}$) and magnetite (Fe_3O_4) were selected as materials. The structure comprises two layers, where YIG microwaveguide lies on the first layer, the waveguide is made in form of elongated strip $L_2 = 4\text{ mm}$ long, $L_1 = 300\ \mu\text{m}$ wide and $b_1 = 10\ \mu\text{m}$ thick. On the second layer at the center of structure in zone $a = 1\text{ mm}$ there are microreservoirs $b_3 = 10\ \mu\text{m}$ thick. Saturation magnetization of YIG is $4\pi M_{YIG} = 1750\text{ G}$, and saturation magnetization of microreservoirs with magnetite is $4\pi M_{\text{chamber}} = 6000\text{ G}$. We studied cases when external magnetic field is directed in positive or negative direction of axis OY . In both cases value of the external magnetic field is $H_0 = 1200\text{ Oe}$.

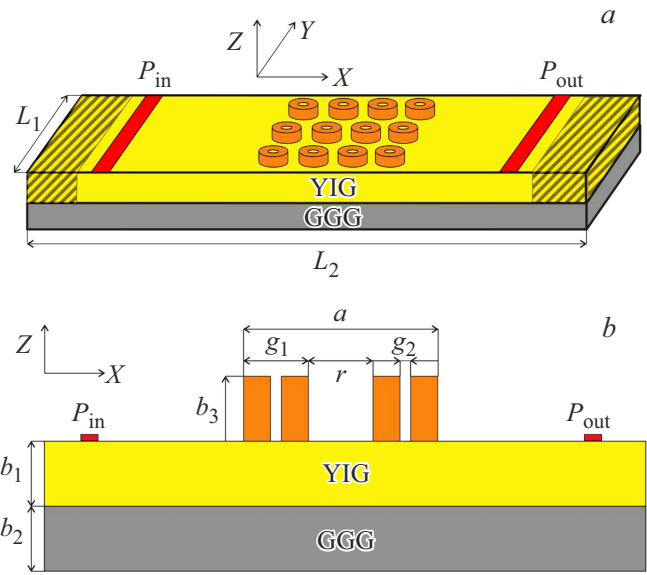


Figure 1. Schematic diagram of structure with microreservoirs (a). The following notations are introduced in the Figure: L_1 — width of microwaveguide, L_2 — length of microwaveguide, P_{in} and P_{out} — microstrip antennas to excite and receive SWs, respectively; (b) schematic image of structure with microreservoirs in plane $Z-X$, where b_1 — thickness of film YIG, b_2 — thickness of film GGG, b_3 — thickness of microreservoir, a — area of microreservoirs application, g_1 — diameter of external ring of microreservoirs, g_2 — diameter of internal ring, r — distance between microreservoirs.

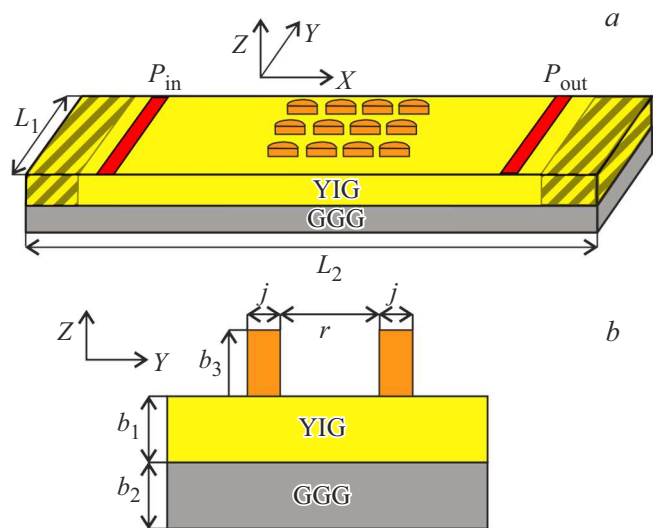


Figure 2. Diagram of structure with microreservoirs (a) in plane $OZ-OY$ (b), where j — diameter of microreservoir, r — distance between microreservoirs.

When solving the problem of spin-wave signal transmission to reduce SWs reflections from boundaries of the design area at boundaries of structure, designated in Figure 1 and Figure 2 by shaded area, the absorbing layers were introduced with exponentially rising decay coefficient α [36–37].

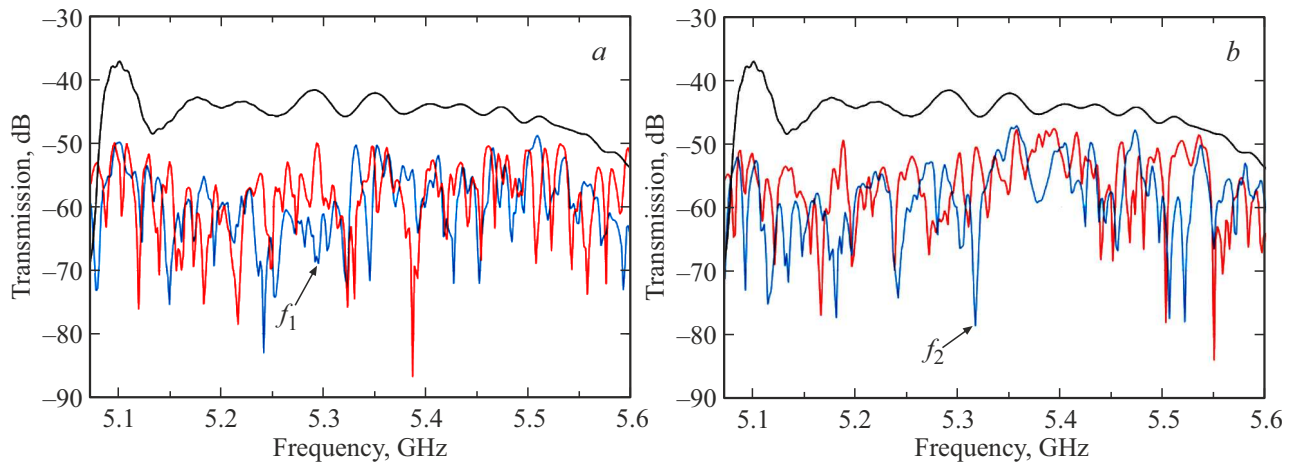


Figure 3. Amplitude-frequency characteristics: (a) for structure shown in Figure 1, (b) for structure shown in Figure 2, taken with P_{out} .

As excitation source of spin-wave signal directly after decay area a microstrip antenna P_{in} $30\ \mu\text{m}$ wide was located, and detecting area P_{out} located at structure output, see Figure 1 and Figure 2.

3. Characteristics of systems YIG/ordered polymer films with magnetic microreservoirs based on micromagnetic modeling

Let's consider operation principle of studied structures: on input antenna P_{in} the microwave signal is applied, its frequency range depends on value of permanent external magnetic field, and from output antenna P_{out} m_z component of magnetization is taken. Using micromagnetic modeling based on solution of Landau–Lifshitz–Hilbert (LLH) equation [38], the modes of SWs spreading in configurations of YIG microwaveguides were studied. LLH equation may be written as:

$$\frac{\partial M}{\partial t} = \gamma [H_{eff} \times M] + \frac{\alpha}{M_s(x,y)} \left[M \times \frac{\partial M}{\partial t} \right], \quad (1)$$

where M — magnetization vector, $\alpha = 10^{-5}$ — decay parameter of film YIG, $H_{eff} = H_0 + H_{demag} + H_{ex} + H_a$ — effective magnetic field, H_0 — external magnetic field, H_{demag} — decay field, H_{ex} — exchange field, H_a — anisotropy field, $\gamma = 2.8\ \text{MHz/Oe}$ — gyromagnetic ratio.

Note that consideration of structure change of internal magnetic field in YIG due to microreservoirs is ensured by consideration of demagnetization field created inside YIG microwaveguide by magnetite localised in microreservoirs.

To analyze effect of the microreservoirs configuration in SW properties in YIG it is important to analyze spectra of VHF signals passage via the studied microwaveguide. For this on the input antenna the magnetic field is set in form

$h = h_0 \sin(2\pi ft)$ with different amplitude of oscillations h_0 and with frequency f .

To obtain information about what happened to the wave after interaction with the system of microreservoirs, the spectral power density of the spin-wave signal was constructed, it was obtained by recording the to file of time realization of the integral value $m_z(x = x_{out}, t)$ for time interval $T_{max} = 300\ \text{ns}$ in area of output antenna at $x = x_{out}$. In Figure 3, *a* the amplitude-frequency characteristic is plotted for structure configuration with polymer ordered microreservoirs with magnetic inclusions, deposited on film YIG, shown in Figure 1, at parameters $g_1 = 20\ \mu\text{m}$, $g_2 = 8\ \mu\text{m}$ and $r = 10\ \mu\text{m}$. In Figure 3, *b* the amplitude-frequency characteristic is plotted for the structure configuration shown in Figure 1, at parameters $j = 10\ \mu\text{m}$, $r = 20\ \mu\text{m}$. Blue curve in Figure 3, (*a*, *b*) corresponds to the case when external magnetic field $H_0 = 1200\ \text{Oe}$ is directed opposite to axis OY , red curve corresponds to the case

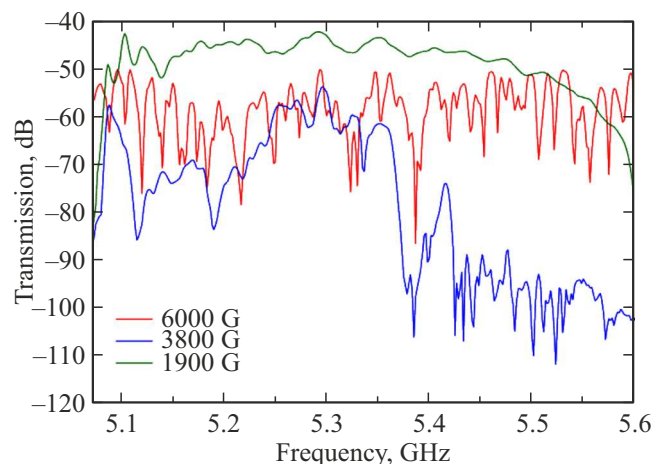


Figure 4. Amplitude-frequency characteristics: for structure with rings at different magnetization of magnetite $4\pi M_{chamber} = 6000\ \text{G}$, $3800\ \text{G}$, $1900\ \text{G}$, taken with P_{out} in case when external magnetic field is oriented in positive direction of axis OY .

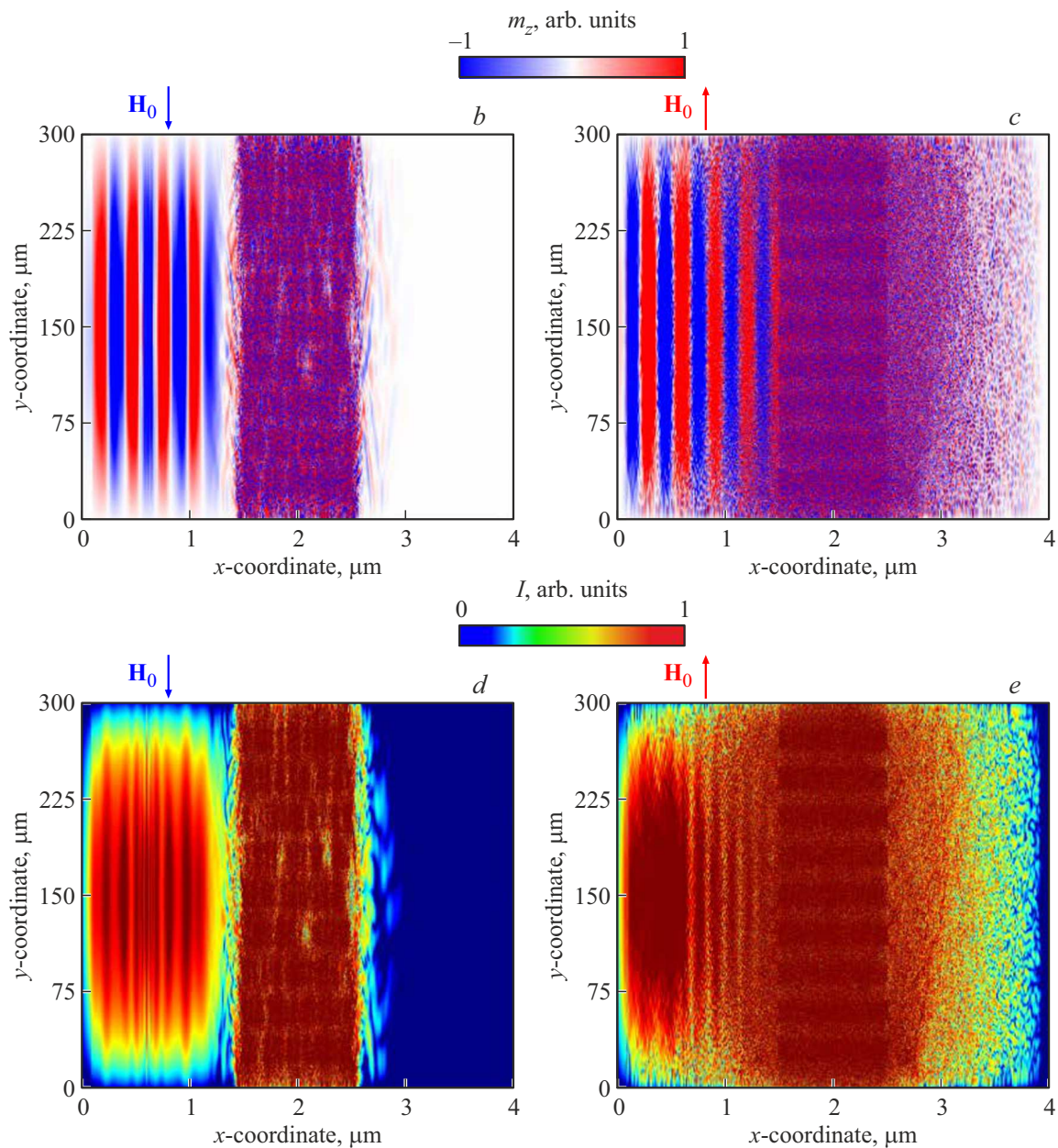


Figure 5. Spatial maps of distribution of m_z component (b, c) and intensity (d, e) of spin waves for structure 1 at frequency f_1 in case of magnetic field oriented in negative (b, d) and positive (c, e) direction of axis OY .

when external magnetic field H_0 is directed along axis OY . The black curve is plotted for the reference microweguide. During modeling the case of reference microweguide was considered for structure configurations at $M_{\text{chamber}} = 0$ G. At that we see that when considering the microweguide with magnetite the level of signal passage decreases by about 20 dB. Also, in frequency dependences of power spectral density we can determine frequencies $f_{1,2}$, when drip is observed at direction change of external bias field.

Note also that changing magnetization of the magnetic material inside the microreservoir $4\pi M_{\text{chamber}}$ we can provide change in nature of SW spreading. For this AFC were plotted for structure in Figure 1, at $4\pi M_{\text{chamber}} = 6000$ G,

3800 G, 1900 G (see Figure 4) if the external magnetic field is 1200 Oe and oriented in positive direction of axis OY . We see that in selected range during value variation of magnetization $4\pi M_{\text{chamber}}$ the narrowing of range of signal passage is observed (blue curve in Figure 4), and areas of signal non-passage occur at the beginning of spectrum of magnetostatic surface waves. When value of magnetization $4\pi M_{\text{chamber}}$ approaches value of magnetization of YIG the frequency band of signal passage occupies the entire frequency range (green curve in Figure 4). At that the selected frequency range 5.07–5.6 GHz corresponds to band of excitation and passage of magnetostatic surface waves upon field increasing 1200 Oe, at that the main effect, confirmed

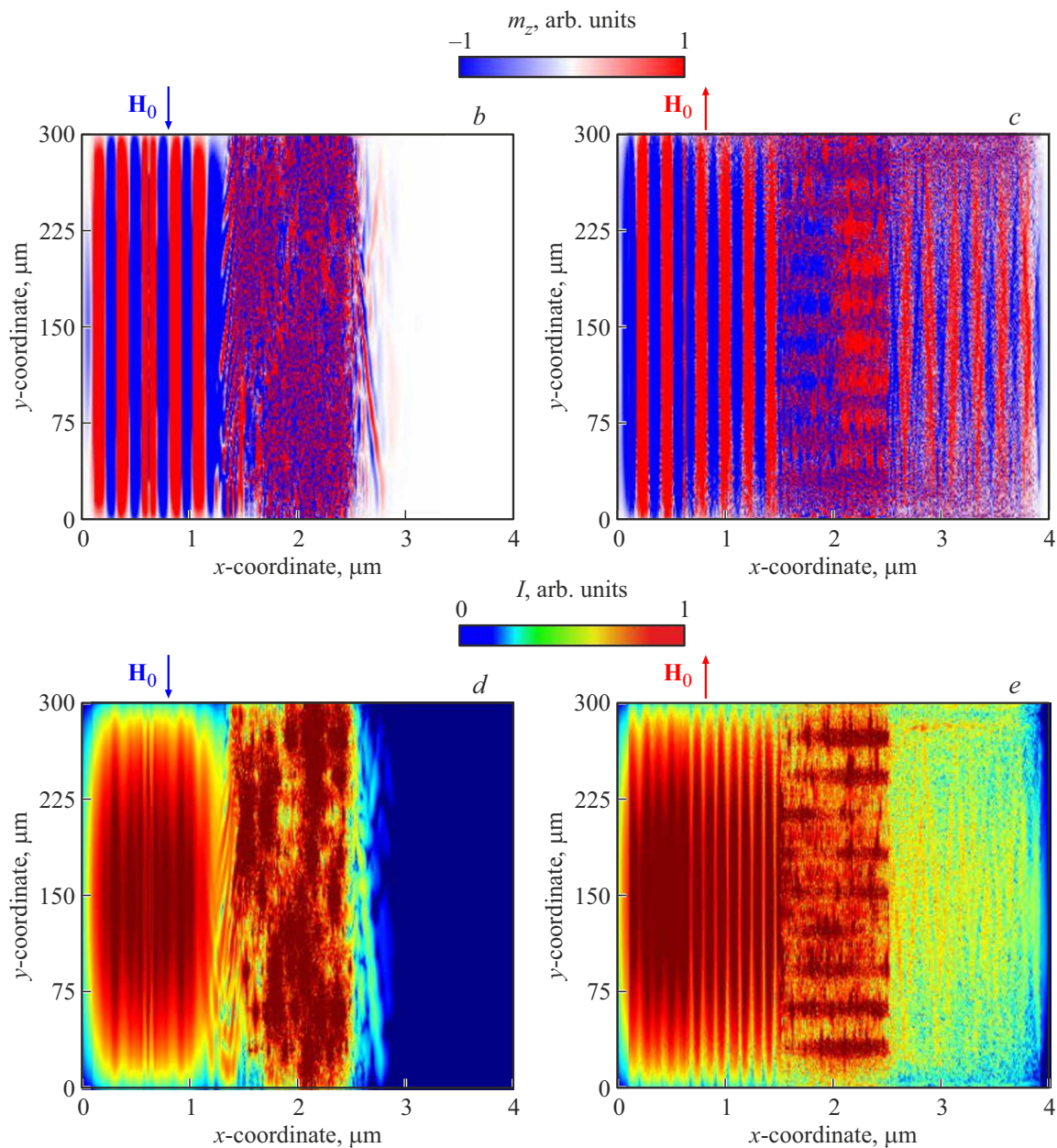


Figure 6. Spatial maps of distribution of m_z component (*b,c*) and intensity (*d,e*) of spin waves for structure 2 (semicylinders) at frequency f_2 in case of magnetic field oriented in negative (*b,d*) and positive (*c,e*) direction of axis OY .

by results of micromagnetic modeling, is observed for the values of the detuning from the ferromagnetic resonance frequency relative to the magnetized film 200 MHz and 300 MHz for frequencies of peaks f_1 and f_2 , respectively.

For the drips observed in amplitude-frequency characteristics the spatial maps were prepared of distribution of m_z component and intensity of spin waves $I = \sqrt{m_z^2 + m_x^2}$ at frequencies $f_1 = 5.295$ GHz for structure shown in Figure 1 (see Figure 5) and at $f_2 = 5.315$ GHz for structure shown in Figure 2 (see Figure 6), when external magnetic field is directed in positive or negative direction of axis OY .

As we can see from the analysis of profiles of magnetization distribution in Figure 5 (*b,d*), SW signal at frequency f_1

at direction of external magnetic field downwards along the axis OY does not pass to the end of structure, and at opposite direction of external magnetic field (see Figure 5 (*c,e*)) it passes, on the contrary. We can conclude that change in direction of the external magnetic field in structure 1 affects the nature of SW spreading. In area after microreservoirs at $x > 2.5$ mm the field distribution indicates that there is no regular wave process after the moment when spin wave passes the are of interaction with microreservoirs.

As we can see from the analysis of profiles of magnetization distribution in Figure 6 (*b,d*), SW signal at frequency f_2 at direction of external magnetic field downwards along the axis OY does not pass to the end of structure, and at oppo-

site direction of external magnetic field (see Figure 6(c,e)) it passes, on the contrary. We can conclude that change in direction of the external magnetic field in structure 2 affects the nature of SW spreading. Moreover note that wave process spreading in area of microreservoirs at $x > 2.5$ mm as per nature of field spreading corresponds to SW excited in area with installed input antenna.

The reservoirs configuration as semicylinders (see Figure 2) ensures the system sensitivity change for sensorics application, at the same time, as it follows from modeling results in Figure 6,e, in linear oriented region between microreservoirs there is spin wave power localization, at that such effect is possible only during reorientation of external field direction. So, we can compare the observed effect with effect of spin wave collimation, described in paper [39]. Number of maxima in the transverse structure of field corresponds to number of rows of microreservoirs. Moreover note that localization is more obvious exactly in case of semicylinders as compared to rings, this is shown by comparison of the results of 2 maps plotting in Figure 5,e and Figure 6,e. Configurations selection of metasurface ensures control of field structure of surface wave, this is important for sensorics applications, their idea is that region filled with bioactive material with microreservoirs can be used as medium with change in magnetic properties due to interaction of introduced chemicals that can change the microreservoirs configuration, and hence the profile of distribution in of magnetic material in form of magnetite nanoparticles located inside the microreservoirs.

In region under microreservoirs there is magnetization distribution close to the case when one wavelength fits along length of this interaction region, at that it is well seen that wavelength excited by antenna is by about 5 times larger than wavelength before the region with microreservoirs. Such difference in wavelengths can be explained by analysis of value of internal field in YIG in region under microreservoirs. Actually, value of internal field reaches 0.8 kOe in region under magnetite, this together with artificially created resonator under the magnetite can be reason of change on spin wavelength. Note that when changing the configuration of magnonic structures with simultaneous variation in the direction of the bias field based on the proposed method of applying microreservoirs filled with magnetite, it may be possible to implement methods for controlling spin-wave signals, which can be applied in magnonic logic and sensoric devices.

4. Conclusion

Thus, study was performed relating the control of the SW characteristics in structure with polymeric planar ordered microreservoirs with magnetic inclusions based on YIG film upon change in the structure parameters, varying the direction of the bias field and change in magnetization value of the magnetic material inside the microreservoir. Spatial maps of distribution of m_z component and intensity of spin

waves are plotted for different structure parameters. It is shown that change in the orientation of the magnetic field to the opposite orientation leads to change in the level of the spin-wave signal passage and the formation of frequency regions on the amplitude-frequency characteristics where the signal stops to spread. The suggested configurations of YIG microwaveguide with system of microreservoirs on surface can be used as orientation controllable magnetic field of VHF signal filter, and to develop new types of biosensors with feedback.

Funding

This study was financially supported by the Russian Science Foundation under project No. 23–13–00373.

Conflict of interest

The authors declare that they have no conflict of interest.

References

- [1] A. Barman, G. Gubbiotti, S. Ladak, A.O. Adeyeye, M. Krawczyk, J. Gräfe, C. Adelman, S. Cotofana, A. Naeemi, V.I. Vasyuchka, B. Hillebrands, S.A. Nikitov, H. Yu, D. Grundler, A.V. Sadovnikov, A.A. Grachev, S.E. Sheshukova, J.-Y. Duquesne, M. Marangolo, G. Csaba, W. Porod, V.E. Demidov, S. Urazhdin, S.O. Demokritov, E. Albisetti, D. Petti, R. Bertacco, H. Schultheiss, V.V. Kruglyak, V.D. Poimanov, S. Sahoo, J. Sinha, H. Yang, M. Mäunzenberg, T. Moriyama, S. Mizukami, P. Landeros, R.A. Gallardo, G. Carlotti, J.-V. Kim, R.L. Stamps, R.E. Camley, B. Rana, Y. Otani, W. Yu, T. Yu, G.E. W. Bauer, C. Back, G.S. Uhrig, O.V. Dobrovolskiy, B. Budinska, H. Qin, S. van Dijken, A.V. Chumak, A. Khitun, D.E. Nikonov, I.A. Young, B.W. Zingsem, M. Winklhofer. *J. of Phys.: Condens. Matter* **33**, 413001 (2021).
- [2] A.G. Gurevich, G.A. Melkov. *Magnetization Oscillations and Waves* CRC-Press, London (1996). 464 p.
- [3] V.E. Demidov and S.O. Demokritov. *IEEE Trans. Magn.* **51**, 1 (2015).
- [4] A.V. Sadovnikov, E.N. Beginin, S.E. Sheshukova, Y.P. Sharavskii, A.I. Stognij, N.N. Novitski, V.K. Sakharov, Y.V. Khivintsev, S.A. Nikitov. *Phys. Rev. B* **99**, 054424 (2019).
- [5] L.D. Landau, E.M. Lifschitz. *Phys. Z. Sowjet.* **8**, 153 (1935).
- [6] S. Demokritov. *Phys. Rep.* **348**, 6, 441 (2001).
- [7] S.O. Demokritov. *SpinWave Confinement: Propagating Waves*, 2nd ed. Jenny Stanford Publishing, N.Y. (2017). 448 p.
- [8] S.L. Vysotskii, Y.V. Khivintsev, V.K. Sakharov, N.N. Novitskii, G.M. Dudko, A.I. Stognii, Y.A. Filimonov. *Phys. Solid State* **62**, 1659 (2020).
- [9] M. Krawczyk, D. Grundler. *J. Phys. Condens. Matter* **26**, 123202 (2014).
- [10] G. Ctistis, E. Papaioannou, P. Patoka, J. Gutek, P. Fumagalli, M. Giersig. *Nano Lett.* **9**, 1, 1 (2009).
- [11] S. Neusser, D. Grundler. *Adv. Mater.* **21**, 2927 (2009).

- [12] X. Zhang. *Mater. Today Electronics* **5**, 100044 (2023).
- [13] I.S. Maksymov, M. Kostylev. *Chemosensors (Basel)* **10**, 49 (2022).
- [14] C. Lueng, P. Lupo, P.J. Metaxas, M. Kostylev, A.O. Adeyeye. *Adv. Mater. Technol.* **1**, 1, 1 (2016).
- [15] C. Lueng, P. Lupo, T. Schefer, P. Metaxas, A. Adeyeye, M. Kostylev. *Int. J. of Hydrogen Energy* **44**, 7715 (2019).
- [16] A.L.R. Souza, M. Gamino, A. Ferreira, A.B. de Oliveira, F. Vaz, F. Bohn, M.A. Correa. *Sensors (Basel)* **21**, 6145 (2021).
- [17] C. Kang, T. Wang, C. Jiang, K. Chen, G. Chai. *J. Alloys Compd.* **865**, 158903 (2021).
- [18] M. Khorshid, P. Losada-Pérez, P. Cornelis, M. Dollt, S. Ingebrandt, C. Glorieux, F.U. Renner, B. van Grinsven, W. De Ceuninck, R. Thoelen, P. Wagner. *Sens. Actuators B Chem.* **310**, 127627 (2020).
- [19] Z. Yang, Y. Liu, C. Lei, X.-C. Sun, Y. Zhou. *Mikrochim. Acta* **182**, 2411 (2015).
- [20] G.V. Kurlyandskaya, M.L. Sánchez, B. Hernando, V.M. Prida, P. Gorria, M. Tejedor. *Appl. Phys. Lett.* **82**, 3053 (2003).
- [21] T. Wang, Z. Yang, C. Lei, J. Lei, Y. Zhou. *Biosens. Bioelectron.* **58**, 338 (2014).
- [22] D. Yu, X. Sun, J. Zou, Z. Wang, F. Wang, K. Tang. *J. of Phys. Chem. B* **110**, 21667 (2006).
- [23] O. Kopach, K. Zheng, O.A. Sindeeva, M. Gai, G.B. Sukhorukov, D.A. Rusakov. *Biomater. Sci.* **7**, 2358 (2019).
- [24] J. Zhang, R. Sun, A.O. DeSouza-Edwards, J. Frueh, G.B. Sukhorukov. *Soft Matter* **16**, 2266 (2020).
- [25] V. Kudryavtseva, M. Otero, J. Zhang, A. Bukatin, D. Gould, G.B. Sukhorukov. *ACS Nanoscience Au* **3**, 3, 256 (2023).
- [26] M.A. Kurochkin, O.A. Sindeeva, A.S. Abdurashitov, N.A. Pyataev, D.A. Gorin, G.B. Sukhorukov. *Biomacromolecules* **24**, 7, 3051 (2023).
- [27] D.T. Simon, S. Kurup, K.C. Larsson, R. Hori, K. Tybrandt, M. Gojny, E.W.H. Jager, M. Berggren, B. Canlon, A. Richter-Dahlfors. *Nature Mater.* **8**, 742 (2009).
- [28] M. Mabrouk, R.M. Abd El-Wahab, H.H. Beherei, M.M. Selim, D.B. Das. *International J. of Pharmaceutics* **587**, 119658 (2020).
- [29] D. Voronin, A. Sadovnikov, D. Shchukin, D.A. Gorin, E. Beginin, Y. Sharaevsky, S. Nikitov. *Tech. Phys. Lett.* **39**, 715 (2013).
- [30] M. Kolasinska, T. Gutberlet, R. Krastev. *Langmuir* **25**, 10292 (2009).
- [31] A.N. Khan, A.V. Ermakov, T. Saunders, H. Giddens, D. Gould, G. Sukhorukov, Y. Hao. *IEEE Sens. J.* **22**, 18162 (2022).
- [32] M.A. Kurochkin, O.A. Sindeeva, A.S. Abdurashitov, N.A. Pyataev, D.A. Gorin, G.B. Sukhorukov. *Biomacromolecules* **24**, 3051 (2023).
- [33] M.A. Kurochkin, O.A. Sindeeva, E.P. Brodovskaya, M. Gai, J. Frueh, L. Su, A. Sapelkin, V.V. Tuchin, G.B. Sukhorukov. *Mater. Sci. Eng. C Mater. Biol. Appl.* **110**, 110664 (2020).
- [34] A.N. Khan, A. Ermakov, G. Sukhorukov, Y. Hao. *Appl. Phys. Rev.* **6**, 041301 (2019).
- [35] S.L. Vysotskiy, Yu.V. Khivintsev, V. Sakharov, Yu. Filimonov. *Tech. Phys.* **64**, 984 (2019).
- [36] G. Venkat, H. Fangohr, A. Prabhakar. *J. Magn. Magn. Mater.* **450**, 34 (2018).
- [37] M. Dvornik, A.N. Kuchko, V.V. Kruglyak. *J. Appl. Phys.* **109**, 07D350 (2011).
- [38] A. Vansteenkiste, J. Leliaert, M. Dvornik, M. Helsen, F. Garcia-Sanchez, B. Waeyenberge. *AIP Advances* **4**, 107133 (2014).
- [39] A.V. Sadovnikov, E.N. Beginin, S.A. Odincov, S.E. Sheshukova, Yu.P. Sharaevskii, A.I. Stognij, S.A. Nikitov. *Appl. Phys. Lett.* **108**, 172411 (2016).

Translated by I.Mazurov